

Alternative Methods of Blackbody Thermodynamic Temperature Measurement Above Silver Point

A. Prokhorov · V. Saprisky · B. Khlevnoy ·
V. Gavrilov

Received: 29 November 2013 / Accepted: 17 December 2014 / Published online: 7 January 2015
© Springer Science+Business Media New York 2015

Abstract Presently, absolute radiometry is the main method of thermodynamic temperature determination above the silver point. The importance of such measurements has increased, as a large international project is underway aimed at assigning thermodynamic temperatures to high-temperature fixed points (HTFPs). All participants are using filter radiometers calibrated against an absolute cryogenic radiometer which, therefore, will be the basis of the provided thermodynamic temperatures of the fixed points. However, such a unified approach may lead to systematic errors (if any) common to all participants. There are methods, providing an alternative to absolute radiometry, which allow the determination of blackbody thermodynamic temperatures using relative measurements. Alternative methods, even if they have lower accuracy than absolute radiometry, could disclose some possible unrecognized systematic errors, or, on the contrary, could confirm the results obtained using absolute radiometry and increase confidence of the thermodynamic temperature determination. One such method, known as the method of ratios (i.e., double wavelength technique), is based on measuring the ratios of fluxes emitted by a blackbody in separate spectral ranges at two temperatures. This approach has been developed at VNIIOFI, but its realization met serious technical difficulties. Modern sensors with improved sensitivity and stability, extremely reproducible HTFP blackbodies, and significant progress in computational methods and computer performance provide a new chance to realize this approach with sufficient accuracy. Another method is based on comparing the ratio of fluxes

A. Prokhorov
Virial International, LLC, 538 Palmspring Dr., Gaithersburg, MD 20878, USA
e-mail: avpro@virial.com

V. Saprisky · B. Khlevnoy (✉) · V. Gavrilov
All-Russian Research Institute for Optical and Physical Measurements (VNIIOFI),
Ozernaya 46, 119361 Moscow, Russia
e-mail: khlevnoy-m4@vniiofi.ru

measured at two wavelengths for a high-temperature blackbody with that measured for synchrotron radiation. This article overviews possibilities of the alternative methods for determination of blackbody thermodynamic temperatures by means of relative radiometry to attract attention of the thermometry and radiometry communities to the importance of international cooperation for realization of these methods.

Keywords Blackbody · Double wavelength technique · High-temperature fixed points · Method of ratios · Synchrotron radiation · Thermodynamic temperature

1 Introduction

Precise determination of the thermodynamic temperature of a blackbody radiator from measurements of its radiation is a problem of great importance for radiation thermometry and blackbody radiometry. This issue has become even more important after the introduction of high-temperature fixed points (HTFPs) in connection with the necessity to assign thermodynamic temperatures to them. In 2007, Working Group 5 of the Consultative Committee for Thermometry (CCT WG5) initiated an international project to assign thermodynamic temperatures to a selected set of HTFPs [1]. The project, whose progress is described in [2], has a final objective to determine definitive thermodynamic temperatures for the melting transitions of the metal–carbon eutectics Co–C (1324 °C), Pt–C (1738 °C), and Re–C (2474 °C) as well as the freezing point of copper by 2015 to make HTFPs routine reference standards for radiation thermometry. This, in turn, can significantly improve the measurement accuracy of radiometric quantities [3].

The usual way to determine the thermodynamic temperature of a high-temperature blackbody, including that based on a HTFP cell, is to measure by a detector the radiant flux emitted by a blackbody and then to calculate the temperature from Planck's law [4–7]. This approach is based on a filter radiometer (FR) and requires absolute measurements of its spectral responsivity and accurate determination of geometrical constants of the optical system selecting the radiation flux. Thermodynamic temperature measurements in such an approach are linked, often via a long traceability chain, to the primary standard of an optical watt—an absolute cryogenic radiometer (ACR), and to the standard of meter through wavelength measurements and geometric measurements of a two-aperture system. One of the largest components in the uncertainty of a FR calibration is the measurement uncertainty of the aperture area of a transfer detector [8].

All national metrology institutes participating in the international project intended to determine thermodynamic temperature of HTFPs, are going to use absolute radiometry, namely, the method based on FR absolutely calibrated against an ACR, because the ACR is considered as the most accurate radiometric instrument and filter radiometry is considered as the most accurate method of blackbody temperature measurement. Therefore, the future high-temperature scale will be based only on absolute radiometric measurements carried out using FRs traceable to the ACR and the length standard.

However, there are alternative approaches to the determination of blackbody temperatures, which are based on relative radiometry methods, namely, the method of

ratios [9–13] and the method of comparing blackbody radiation with that of a synchrotron [14]. Since these methods use only ratios of detector signals, absolute calibration of detectors in terms of radiometric units is not required. The main requirement for the detectors used is the linearity of their responses. Under certain conditions, these methods allow avoiding measurements of some physical quantities (including aperture areas) whose accuracy is otherwise critical for the accuracy of the measured temperature.

Even if these methods are less accurate than absolute radiometry, alternative approaches employing different measurement principles, could detect possible unrecognized systematic errors (if any), which should be common for all implementations of the absolute radiometry method, or, on the contrary, confirm their results and, suchwise, increase confidence of the thermodynamic temperature measurements.

In this paper, we overview the possibilities and prospects of relative radiometry application to the blackbody temperature determination in order to attract attention of radiometric and thermometric communities to the importance of international cooperation for realizing alternative methods.

2 Methods of Ratios

2.1 Background

One of the most promising approaches based on relative radiometric measurements implies determining the ratios of radiometric quantities of blackbody radiation at two temperatures. Often, it is referred to as “the method of ratios”. To our knowledge, it was proposed for the first time by Wulfson in his paper “Absolute Method of Blackbody Temperatures Measurement” published in Russian in 1951 [9]. Therefore, the method is also known as Wulfson’s method. Realization of this method does not require calibration of a detector in absolute units; the main requirement imposed is the linearity of the detector response. Since relative measurements are easier in implementation and can be performed with better precision than absolute measurements, the method of ratios looks very attractive. It is based on measurement of ratios X_1 and X_2 of spectral radiances (or irradiance, or other radiometric quantity) of a perfect blackbody at two known wavelengths, λ_1 and λ_2 , and two temperatures, T_1 (thermodynamic temperature that has to be determined) and T_2 (that is considered as an auxiliary temperature):

$$X_1 = \left[\exp \left(\frac{c_2}{\lambda_1 T_2} \right) - 1 \right] \cdot \left[\exp \left(\frac{c_2}{\lambda_1 T_1} \right) - 1 \right]^{-1}, \quad (1a)$$

$$X_2 = \left[\exp \left(\frac{c_2}{\lambda_2 T_2} \right) - 1 \right] \cdot \left[\exp \left(\frac{c_2}{\lambda_2 T_1} \right) - 1 \right]^{-1}, \quad (1b)$$

where $c_2 \approx 1.4388 \times 10^4 \mu\text{m}\cdot\text{K}$ is the second radiation constant in Planck’s law. Here and hereinafter, we will assume that measurements are conducted in vacuo; if the measurements are conducted in a gaseous medium, a correction for its refractive index can easily be made following [15].

Equations 1a and 1b must be solved together for T_1 and T_2 . Apparently, realizing the difficulties of solving this system of nonlinear equations, Wulfson [9] proposed to choose temperatures and wavelengths in such a way that the Wien approximation would be valid for the first ratio, while the Rayleigh–Jeans law could be applied for the second ratio. In this case, T_1 and T_2 can be found analytically. Along with the limitations associated with the choice of temperature and wavelength ranges, this method could only provide an accuracy worse than that achievable by usual pyrometric means and was forgotten for a long time. However, Eqs. 1a and 1b themselves encompass the reasonable idea: the Planckian radiator allows the determination of its thermodynamic temperature on the basis of relative measurements (only wavelength measurements have to be absolute).

Another approach employs the ratio X of spectral radiances at a known wavelength λ_0 and the ratio Z of radiant exitances of a blackbody at temperatures T_1 and T_2 [16]. Using the Planck and Stefan–Boltzmann laws, one can write the system of nonlinear equations:

$$X = \left[\exp\left(\frac{c_2}{\lambda_0 T_2}\right) - 1 \right] \cdot \left[\exp\left(\frac{c_2}{\lambda_0 T_1}\right) - 1 \right]^{-1}, \tag{2a}$$

$$Z = (T_1/T_2)^4. \tag{2b}$$

If λ_0 , T_1 , and T_2 are chosen in such a way that the Wien approximation is sufficiently accurate, Eqs. 2a and 1b can be solved for T_1 and T_2 analytically; otherwise, they must be solved numerically. It was assumed that the ratio X can be measured using a monochromator and a linear detector, while a linear non-selective thermal detector should be used to measure the ratio Z . Needless to say, this approach is idealized: the finite bandwidth of a monochromator and residual selectivity of a thermal detector are the main sources of uncertainties. Nonetheless, comparative analysis of various ratios methods [11, 17] shows that, for the best estimation, they allow measurements of the thermodynamic temperatures of blackbodies with an uncertainty of the order of 1 K at about 3000 K.

The advent of precision FRs opens up new perspectives for the method of ratios. At NPL, application of two FRs with known relative spectral responsivities, $r_1(\lambda)$ and $r_2(\lambda)$, for the determination of thermodynamic temperatures was analyzed by computer modeling [12]. For this method, referred to as “the double-wavelength technique,” the following system of equations can be written:

$$X_1 = \left[\int_0^\infty \frac{r_1(\lambda) d\lambda}{\lambda^5 \left[\exp\left(\frac{c_2}{\lambda T_1}\right) - 1 \right]} \right] \cdot \left[\int_0^\infty \frac{r_1(\lambda) d\lambda}{\lambda^5 \left[\exp\left(\frac{c_2}{\lambda T_2}\right) - 1 \right]} \right]^{-1}, \tag{3a}$$

$$X_2 = \left[\int_0^\infty \frac{r_2(\lambda) d\lambda}{\lambda^5 \left[\exp\left(\frac{c_2}{\lambda T_1}\right) - 1 \right]} \right] \cdot \left[\int_0^\infty \frac{r_2(\lambda) d\lambda}{\lambda^5 \left[\exp\left(\frac{c_2}{\lambda T_2}\right) - 1 \right]} \right]^{-1}. \tag{3b}$$

As is easily seen, Eqs. 3a and 3b are the generalization of systems of Eqs. 1a and 1b and 2a and 2b: if $r_1(\lambda) = \delta(\lambda - \lambda_1)$ and $r_2(\lambda) = \delta(\lambda - \lambda_2)$, Eqs. 3a and 1b become

equivalent to Eqs. 1a and 1b; if $r_1(\lambda) = \delta(\lambda - \lambda_0)$ and $r_2(\lambda) \equiv 1$, Eqs. 3a and 1b take the form of Eqs. 2a and 1b (here, δ is the Dirac delta function). In [12], recovery of $T_1 = 2747$ K (the melting temperature of Re–C eutectic) and $T_2 = 1357.77$ K (the freezing temperature of Cu) was modeled; it was supposed that the ratio X_1 is obtained using the FR with a silicon photodiode and $r_1(\lambda)$ centered at $0.7 \mu\text{m}$; X_2 is obtained using the FR with an InSb sensor and $r_2(\lambda)$ centered at $4.55 \mu\text{m}$. The FRs' bandpasses were specified as 3 nm and 85 nm, respectively. Evaluation of uncertainties of T_1 and T_2 recovery from computed values of X_1 and X_2 was performed by adding multiplicative Gaussian noise to X_1 and X_2 and employing Monte Carlo modeling of uncertainty propagation according to JCGM 101:2008 [18]. It was concluded that, at realistic values of affecting factors and rather optimistic than realistic values of measurement uncertainties, the melting temperature of the Re–C eutectic can be determined with a standard uncertainty of about 0.5 K.

Recently, Saunders [13] applied the Sakuma–Hattori approximation [19,20] of Planck's law to derive analytical expressions for standard uncertainties of the determination of thermodynamic temperatures by the double-wavelength technique and performed a detailed analysis for the comparison of HTFP blackbodies with blackbodies at fixed points of the ITS-90. An important conclusion was drawn on the approach to minimize these uncertainties: the two FRs must have spectral responsivities very different in width while their center wavelengths do not necessarily have to be widely separated. It was noted in [13] that although the Sakuma–Hattori approximation is adequate to be used for analysis of uncertainty propagation, the unknown temperatures T_1 and T_2 must be determined by direct solution of Eqs. 3a and 1b. The Levenberg–Marquardt (LM) nonlinear least-squares fitting algorithm [21] was proposed for their solution.

2.2 Solution of the System of Governing Equations

The most common approach to solution of the system of nonlinear equations is to reduce this problem to the equivalent problem of minimization of the Euclidean distance between an initial guess and the true solution. For Eqs. 3a and 1b, such an approach leads to the minimization problem for the objective function,

$$F(T_1, T_2) = [X_{1,\text{true}} - X_1(T_1, T_2)]^2 + [X_{2,\text{true}} - X_2(T_1, T_2)]^2, \quad (4)$$

where T_1 and T_2 are unknown temperatures that have to be found; $X_{1,\text{true}}$ and $X_{2,\text{true}}$ are the signal ratios computed according to Eqs. 3a and 1b for the true blackbody temperatures $T_{1,\text{true}}$ and $T_{2,\text{true}}$, respectively.

Since one of our goals was to assess the feasibility of the method of ratios realized using one photodetector and two filters having very different bandwidths, we chose for modeling the well-studied Hamamatsu S1337 silicon photodiode with two filters: the first, a narrow-band interference filter with the Gaussian spectral transmittance centered at 650 nm and an FWHM of 10 nm, and the second, a wide-band Schott KG5 glass filter [22]. Relative spectral responsivities of these two FRs with the same photodiode but different filters are shown in Fig. 1. Hereinafter, all numerical examples

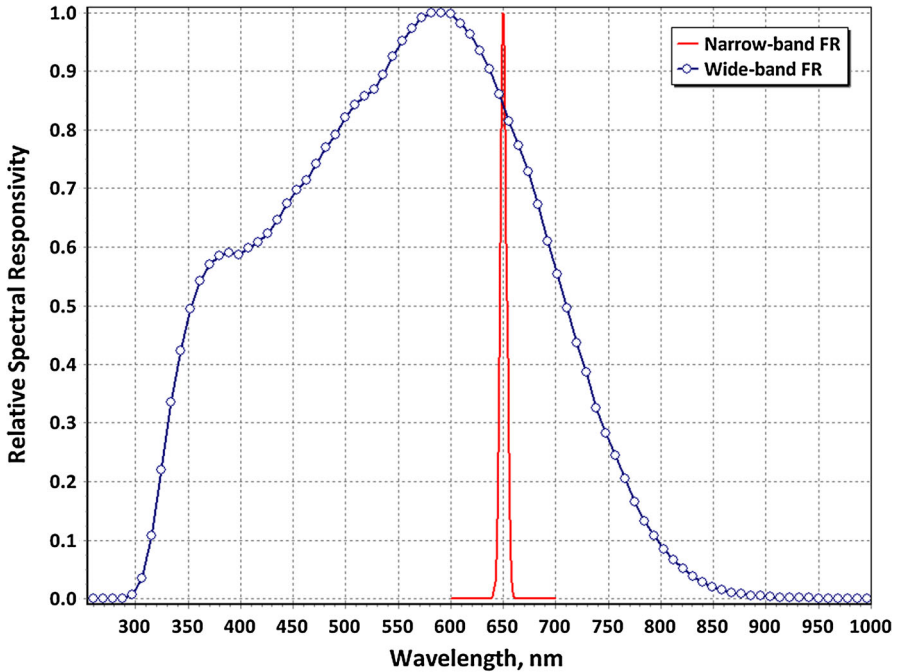


Fig. 1 Relative spectral responsivities of two filter radiometers with silicon photodiodes

are provided for this case. Figure 2 presents the surface of $F(T_1, T_2)$ for $T_{1,\text{true}} = 1357.77$ K (the freezing temperature of copper) and $T_{2,\text{true}} = 2747$ K (the melting temperature of Re–C eutectic alloy) plotted on a logarithmic scale within the square $100 \text{ K} \times 100 \text{ K}$ using a regular grid with 2001×2001 nodes. We chose this pair of temperatures to maintain the comparability with the results provided in [12]. Actually, the method of ratios is equally applicable to fixed-point and variable-temperature blackbodies; the surface plot corresponding to the pyrolytic graphite blackbody [23] at temperatures $T_{1,\text{true}} = 2500$ K and $T_{2,\text{true}} = 3500$ K is presented in Fig. 3. Both surfaces have a similar shape: the very narrow deep minimum ($F = 0$; $\lg(F) = -\infty$) corresponds to $T_1 = T_{1,\text{true}}$ and $T_2 = T_{2,\text{true}}$ lies at the bottom of a narrowing down valley.

Minimization of $F(T_1, T_2)$ requires application of appropriate numerical methods. Initially, we applied the algorithm of particle swarm optimization (PSO) [24]. PSO is a derivative-free, stochastic optimization method that mimics random movement of “particles” in a multidimensional (two-dimensional, in our case) search space. The swarm is initialized by particles randomly distributed over the search space. The movements of the particles are determined by their individual best-known positions and the best-known position for a swarm as a whole. PSO does not require a “good” initial guess but needs only to specify the boundary of the search space. We achieved reliable determination of the global minimum even for a very large search range ($400 \text{ K} \leq T_1, T_2 \leq 4000 \text{ K}$) after several restarts of the PSO search algorithm. However, the PSO

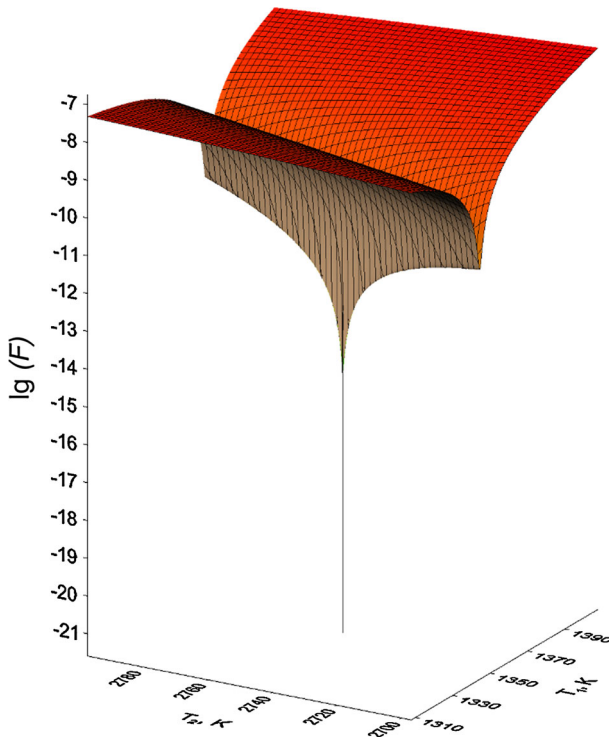


Fig. 2 Three-dimensional (3D) plot of the objective function $F(T_1, T_2)$ for $T_{1,\text{true}} = 1357.77$ K and $T_{2,\text{true}} = 2747$ K

method, especially with application of a multi-restart strategy, is too slow for evaluation of uncertainty propagation via Monte Carlo modeling according to [18]. For this reason, we finally adopted one of the LM algorithms from the MINPACK-1 Fortran 77 library developed at the Argonne National Laboratory [25]. The convergence domain is large enough although it depends on initial settings (conditions of the iterative process termination, initial step bound, and the mode of variables scaling). No problems with convergence arise if an initial guess is chosen in such a way that the first (smaller) of the starting temperatures is less than $\min(T_{1,\text{true}}, T_{2,\text{true}})$ while the second (larger) starting temperature is greater than $\max(T_{1,\text{true}}, T_{2,\text{true}})$. For most cases, the solution is obtained almost instantaneously, after several iterations.

2.3 Evaluation of Solution Stability

Numerical experiments with the pairs of above-mentioned temperatures showed that solution of Eqs. 1a and 1b is unstable: even small changes in X_1 or X_2 may result in significant changes in T_1 and T_2 . All other things being equal, solution of Eqs. 2a and 1b is stable enough: uncertainties in the thermodynamic temperature determination depend almost linearly on the uncertainty of the less precise FR for the signal

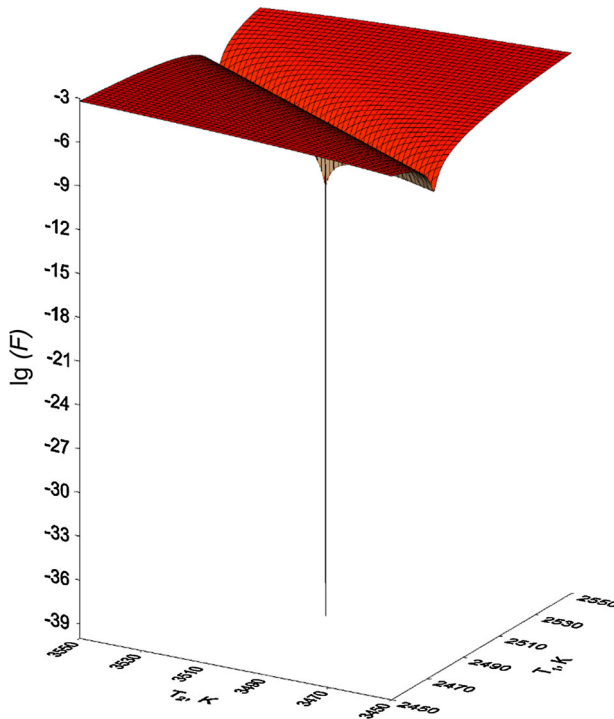


Fig. 3 3D plot of the objective function $F(T_1, T_2)$ for $T_{1,\text{true}} = 2500$ K and $T_{2,\text{true}} = 3500$ K

uncertainties that ranged from 0.01 % to 0.5 %. Solution of Eqs. 3a and 3b has an intermediate stability that depends to a great extent upon the spectral responsivity curves of both FRs. Numerical experiments confirmed the conjecture made in [13] that the use of two FRs with spectral bands very different in width (in contrast to two narrow-band FRs in [12]) can improve the solution stability for Eqs. 3a and 3b.

We performed the Monte Carlo modeling to assess the stability of solutions to the random errors added to measured signals unlike [12], where such errors were added to the ratio values. For numerical experiments, $X_{1,\text{true}}$ and $X_{2,\text{true}}$ were pre-computed for the known (true) values of $T_{1,\text{true}}$ and $T_{2,\text{true}}$; the same $r_1(\lambda)$, and $r_2(\lambda)$ depicted in Fig. 1 were used for all cases. We assumed that the output signal of FRs can be measured with an uncertainty characterized by the Gaussian probability distribution with a zero mean and a standard deviation of 0.01 %.

Figures 4 and 5 present the scatter plots of errors $T_1 - T_{1,\text{true}}$ and $T_2 - T_{2,\text{true}}$ obtained after 10 000 trials for $(T_{1,\text{true}} = 1357.77$ K, $T_{2,\text{true}} = 2747$ K) and $(T_{1,\text{true}} = 2500$ K, $T_{2,\text{true}} = 3500$ K), respectively. The signals $S_{\text{FR1}}(T_{1,\text{true}})$, $S_{\text{FR1}}(T_{2,\text{true}})$, $S_{\text{FR2}}(T_{1,\text{true}})$, and $S_{\text{FR2}}(T_{2,\text{true}})$ were computed by numerical integration of appropriate Planckian functions multiplied by relative spectral responsivities; then the multiplicative random Gaussian error with a standard deviation of 0.01 % was added to each signal and the ratios were computed. For each pairs of X_1 and X_2 obtained in such a way, T_1 and T_2 were found by the LM method. The mean

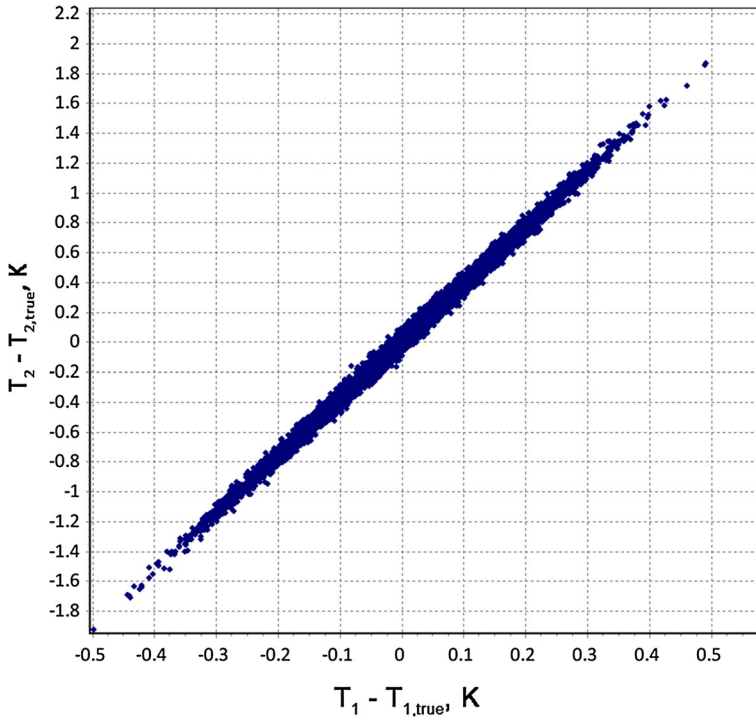


Fig. 4 Scatter plot of errors in calculations of T_1 and T_2 for $T_{1,\text{true}} = 1357.77$ K and $T_{2,\text{true}} = 2747$ K, and a standard uncertainty of signal measurement of 0.01 %

values of T_1 and T_2 , standard uncertainties $u(T_1)$ and $u(T_2)$, and correlation coefficient $r(T_1, T_2)$ computed by statistical processing of the modeling results are collected in Table 1. In both cases, the correlation coefficients $r(T_1, T_2)$ are very close to unity. This means that there is almost a linear dependence between $u(T_1)$ and $u(T_2)$, in accordance with the well-known approximate equation (see, e.g., [8]):

$$u(T_2) = \left(\frac{T_2}{T_1}\right)^2 u(T_1). \quad (5)$$

We found that the standard uncertainties up to 0.05 nm in wavelength measurements (rectangular probability distribution was modeled) and up to 0.05 % in determination of the relative spectral responsivities (Gaussian probability distributions were modeled) affect weakly computed temperatures and their uncertainties. We would emphasize that the uncertainties evaluated constitute only a part of the uncertainty budget; the model we built does not include uncertainties associated with a particular hardware implementation. Although these results can be considered only as preliminary, the method of ratios seems to be very promising.

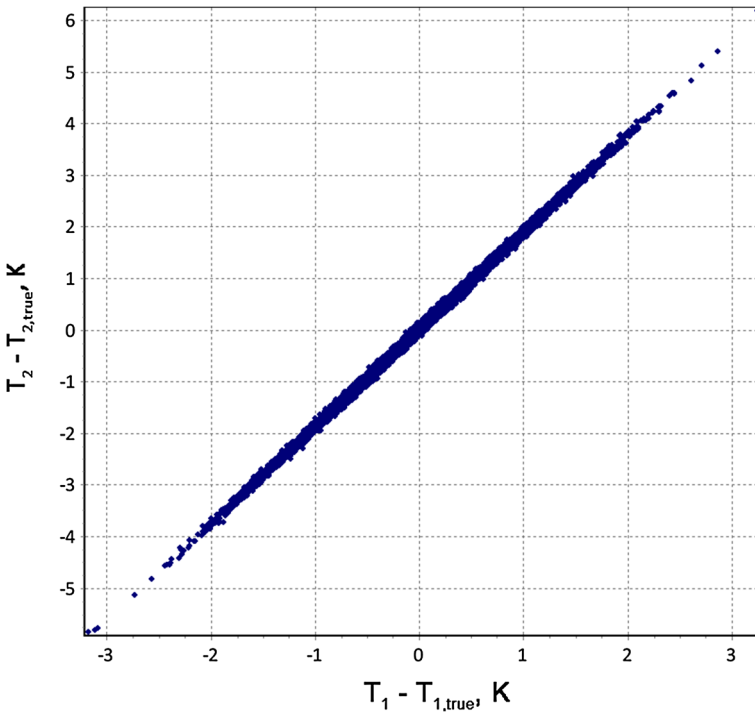


Fig. 5 Scatter plot of errors in calculations of T_1 and T_2 for $T_{1,true} = 2500$ K and $T_{2,true} = 3500$ K, and a standard uncertainty of signal measurement of 0.01 %

Table 1 Results of Monte Carlo modeling of uncertainty propagation for the method of ratios

$T_{1,true}$ and $T_{2,true}$ (K)	T_1 and T_2 (K)	$u(T_1)$ (mK)	$u(T_2)$ (mK)	$r(T_1, T_2)$	$\left(\frac{T_{2,true}}{T_{1,true}}\right)^2$	$\frac{u(T_2)}{u(T_1)}$
1357.77 and 2747	1357.768 and 2746.994	130	497	0.9978	4.093	3.823
2500 and 3500	2500.002 and 3500.004	781	1472	0.9994	1.960	1.885

3 Blackbody Versus Synchrotron

Another method of relative radiometry has been proposed in [14]. Its essence is in comparing the ratios of irradiances produced at two wavelengths by the thermal radiation of a high-temperature blackbody and the synchrotron radiation of an electron storage ring, two standard sources based on different fundamental physical laws. An intuitive premise of this method is a strong dependence of the blackbody relative spectrum on its temperature and, on the other hand, a weak dependence of the synchrotron radiation spectrum on storage ring parameters in the visible spectral range. The original work [14] considered the monochromatic Wien’s approximation; relative spectral responsivities $r_1(\lambda_1)$ and $r_2(\lambda_2)$ of the detector(s) are supposed to be unknown. If the measurement geometry and the blackbody spectral effective emissivity are identical

at λ_1 and λ_2 , one can write the ratio X of the blackbody irradiances using Planck's law:

$$X = \frac{S_{\text{BB}}(\lambda_1)}{S_{\text{BB}}(\lambda_2)} = \frac{r_1(\lambda_1)}{r_2(\lambda_2)} \left(\frac{\lambda_2}{\lambda_1}\right)^5 \frac{\exp\left(\frac{c_2}{\lambda_2 T}\right) - 1}{\exp\left(\frac{c_2}{\lambda_1 T}\right) - 1}, \quad (6)$$

where $S_{\text{BB}}(\lambda_1)$ and $S_{\text{BB}}(\lambda_2)$ are the measured signals at the wavelengths λ_1 and λ_2 , respectively.

The second ratio is obtained from measurements at the same wavelengths of the spectral irradiance produced by the synchrotron radiation. If one assumes the measurement geometry to be identical for measurements at both wavelengths (although this geometry may not necessarily coincide with that at the blackbody measurements), one can write

$$Y = \frac{r_1(\lambda_1) E_{\lambda, \text{SR}}(\lambda_1)}{r_2(\lambda_2) E_{\lambda, \text{SR}}(\lambda_2)}. \quad (7)$$

The spectrum of the synchrotron radiation can be computed on the basis of the classical Schwinger theory for the accelerated relativistic electron [26]. The continuous spectrum of the synchrotron radiation is divided by the so-called critical wavelength λ_c into two parts: half of the power is radiated above λ_c and half below. The critical wavelength is expressed as follows:

$$\lambda_c = \gamma^{-3} \frac{4\pi R}{3}, \quad (8)$$

where $\gamma = E/(m_0 c^2)$; E and m_0 are the electron energy and rest mass, respectively; c is the speed of light; and R is the curvature radius of the electrons' orbit.

The synchrotron radiation is highly collimated; its peak corresponds to a direction tangential to the particle orbit. Integration of the Schwinger equation over all directions perpendicular to the electron orbital plane allows application to Eq. 8 the well-known approximation for $\lambda \gg \lambda_c$ (see, e.g., [27]) that is based on the asymptotic behavior of the modified Bessel functions of the second kind:

$$Y = \frac{r_1(\lambda_1)}{r_2(\lambda_2)} \left(\frac{\lambda_1}{\lambda_2}\right)^{-7/3}. \quad (9)$$

There are two conditions for validity of Eq. 9: (i) all the radiation spread in the direction perpendicular to the electron orbital plane must be collected and (ii) both wavelengths λ_1 and λ_2 must be much larger than the critical wavelength λ_c .

Fulfillment of the first condition is not a complex problem because the synchrotron radiation beam in the direction perpendicular to the electron orbital plane has a very small half-opening angle given by $\Delta\psi/2 = \gamma^{-1}$. For instance, the electron energy of 500 MeV gives $\Delta\psi/2 \approx 1$ mrad. The modern measurement facilities on the base of the electron storage ring allow employing the aperture of about 3 mm to 5 mm

in diameter to measure the irradiance of the synchrotron radiation in the visible and near-IR spectral ranges [28,29].

The second condition can also be easily fulfilled. For instance, for the metrology light source (MLS), the electron storage ring of the Physikalisch-Technische Bundesanstalt (PTB, Germany), the critical wavelength λ_c at 630 MeV energy is equal to 3.4 nm [30]. At this electron energy, the spectral irradiance level in the visible and near infrared spectral ranges can be made comparable with that of a blackbody at 3000 K by adjustment of the electron beam current.

Using Eqs. 7 and 10, we can form the ratio $A = Y/X$:

$$A = \left(\frac{\lambda_1}{\lambda_2}\right)^{\frac{8}{3}} \frac{\exp\left(\frac{c_2}{\lambda_1 T}\right) - 1}{\exp\left(\frac{c_2}{\lambda_2 T}\right) - 1} \tag{10}$$

If the wavelengths λ_1 and λ_2 are known and the ratios X and Y are determined as described above, we can compute the constant A and solve Eq. 10 for the unknown temperature T . The easiest way to find the single root of this nonlinear equation is to use a bisection-like method, e.g., the Brent method [31], which allows obtaining the solution almost instantaneously.

Over almost two decades that elapsed since publication of the paper in [14], important changes have taken place in optical radiometry. First, the FRs operating in the irradiance mode and having unprecedented accuracy which is limited primarily by the uncertainty in measurement of aperture areas were introduced in metrological practice. Second, the MLS, a synchrotron radiation source with a reduced electron energy dedicated to synchrotron-radiation-based metrology throughout the optical spectral range was commissioned in 2008 [32]. Third, the very stable high-temperature pyrolytic graphite blackbodies were developed, including those capable to serve as heating furnaces for large-aperture HTFP cells such as eutectic Re–C (2747 K) or peritectic WC–C (3022 K) were developed [23]. Taking into account these achievements, the method of comparing the ratios of blackbody and synchrotron radiation can be adopted to operations with the FRs having the relative spectral responsivities $r_1(\lambda)$ and $r_2(\lambda)$. Equation 10 should be re-written in the form,

$$A = \frac{\int_0^\infty \lambda^{-7/3} r_1(\lambda) d\lambda}{\int_0^\infty \lambda^{-7/3} r_2(\lambda) d\lambda} \cdot \frac{\int_0^\infty \lambda^{-5} r_2(\lambda) [\exp\left(\frac{c_2}{\lambda T}\right) - 1]^{-1} d\lambda}{\int_0^\infty \lambda^{-5} r_1(\lambda) [\exp\left(\frac{c_2}{\lambda T}\right) - 1]^{-1} d\lambda}, \tag{11}$$

if the asymptotic expression for $\lambda \gg \lambda_c$ is used, or in the form,

$$A = \frac{\int_0^\infty E_{\lambda, sr}(\lambda) r_1(\lambda) d\lambda}{\int_0^\infty E_{\lambda, sr}(\lambda) r_2(\lambda) d\lambda} \cdot \frac{\int_0^\infty \lambda^{-5} r_2(\lambda) [\exp\left(\frac{c_2}{\lambda T}\right) - 1]^{-1} d\lambda}{\int_0^\infty \lambda^{-5} r_1(\lambda) [\exp\left(\frac{c_2}{\lambda T}\right) - 1]^{-1} d\lambda}, \tag{12}$$

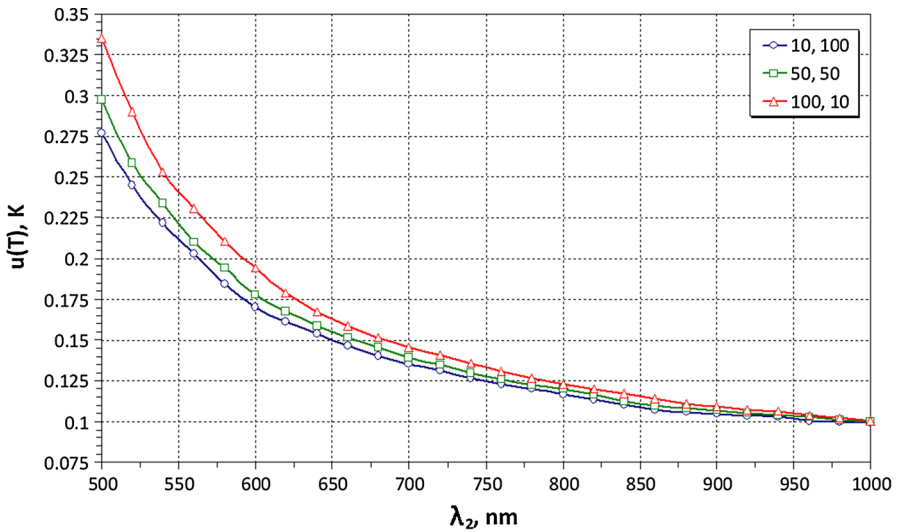


Fig. 6 Dependence of the uncertainty $u(T)$ of the recovered blackbody temperature $T = 3000$ K on the center wavelength λ_2 ; the center wavelength $\lambda_1 = 400$ nm; the standard uncertainty of signal measurements is 0.01 %. Numbers separated by a comma in the legend indicate $\Delta\lambda_1$ and $\Delta\lambda_2$ in nm

if calculation of $E_{\lambda,SR}(\lambda)$ using Schwinger's theory and absolute measurement of the electron storage ring operational parameters [33] provides higher accuracy.

To evaluate the feasibility of realization of this method using the FR technique, we performed numerical modeling of a simple case, when the blackbody has a temperature of 3000 K, the two FRs have rectangular relative spectral responsivities with center wavelengths and widths λ_1 , $\Delta\lambda_1$ and λ_2 , $\Delta\lambda_2$, respectively. It was assumed that $\lambda_1 = 400$ nm while λ_2 varies from 500 nm to 1000 nm. Various combinations of widths of 10 nm, 50 nm, and 100 nm for $\Delta\lambda_1$ and $\Delta\lambda_2$ were studied. For all four signals included in Eq. 11, we modeled the uncorrelated multiplicative random errors with a Gaussian probability distribution, zero mean and relative standard deviations σ_S of 0.01 % and 0.02 %. Some results for the standard uncertainties $u(T)$ are plotted against λ_2 in Fig. 6 (for $\sigma_S = 0.01$ %) and 7 (for $\sigma_S = 0.02$ %). Each value of $u(T)$ was computed using 10 000 random trials. The numbers separated by a comma in the legends indicate $\Delta\lambda_1$ and $\Delta\lambda_2$ in nm. According to Figs. 6 and 7, the standard uncertainty $u(T)$ depends more strongly on the distance between center wavelengths λ_1 and λ_2 than on the bandwidths $\Delta\lambda_1$ and $\Delta\lambda_2$; however, for every σ_S (and, apparently, the lower wavelength λ_1), there is a lower bound, to which $u(T)$ approaches asymptotically, so that a further increase in the distance between λ_1 and λ_2 does not lead to a noticeable decrease of $u(T)$. The modeling results give hope to the possibility of implementation for this method using FRs with silicon photodiodes.

Again, it should be noted that the uncertainties evaluated are not the total uncertainties in the blackbody temperature determination. Other sources of errors can be included in the model when a particular hardware implementation will be defined. The blackbody temperature can be determined using measurements at only two wavelengths, but comparison of measurements carried out at several different wavelengths can help to identify some possible unrecognized systematic errors.

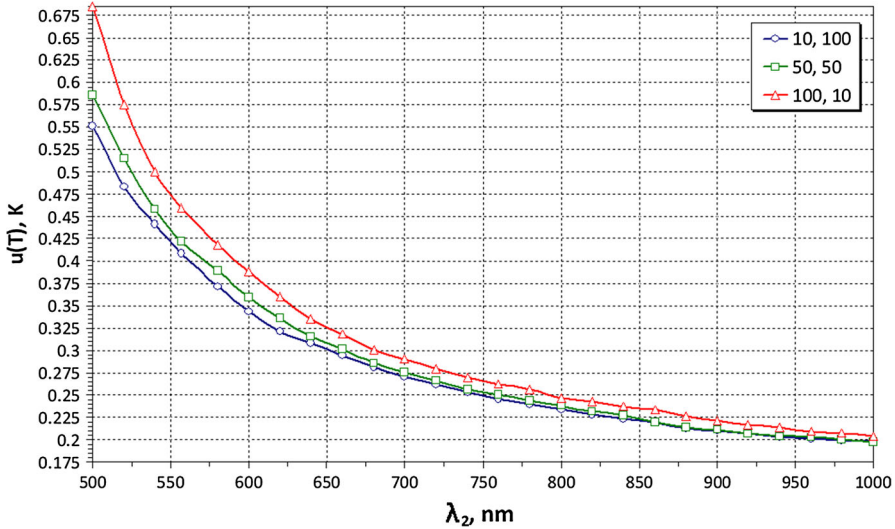


Fig. 7 Dependence of the uncertainty $u(T)$ of the recovered blackbody temperature $T = 3000$ K on the center wavelength λ_2 ; the center wavelength $\lambda_1 = 400$ nm; the standard uncertainty of signal measurements is 0.02 %. Numbers separated by a comma in the legend indicate $\Delta\lambda_1$ and $\Delta\lambda_2$ in nm

4 Conclusion

In this paper, methods for determination of the high-temperature blackbody thermodynamic temperature, which are based on relative radiometry were considered as a necessary alternative (but not a replacement) to the method based on absolute radiometry and linked to the primary cryogenic radiometer. Realization of the relative radiometry methods allows comparisons of two branches of radiometry—detector-based, which uses the ACR as a primary standard, and source-based, which employs the blackbody and/or electron storage ring.

Alternative methods employing different measurement principles can increase the confidence in the high-temperature scale, even if they cannot compete in precision with the absolute radiometry methods. Unprecedented stability achieved for HTFP blackbodies and progress in filter radiometry allow one to make a reassessment of the relative radiometry importance for determination of thermodynamic temperatures of blackbodies above the silver point.

Acknowledgment The work was carried out with the financial support of the Ministry of Education and Science of the Russian Federation.

References

1. G. Machin, P. Bloembergen, J. Hartmann, M. Sadli, Y. Yamada, *Int. J. Thermophys.* **28**, 1976 (2007)
2. G. Machin, K. Anhalt, P. Bloembergen, M. Sadli, Y. Yamada, E. Woolliams, in *Proceedings of Ninth International Temperature Symposium* (Los Angeles), *Temperature: Its Measurement and Control*, ed.

- by C.W. Meyer. Science and Industry, vol. 8, A.I.P. Conference Proceedings 1552 (AIP, Melville, NY, 2013), pp. 317–322
3. Y. Yamada, B. Khlevnoy, Y. Wang, T. Wang, K. Anhalt, Metrologia **43**, S140 (2006)
 4. G. Machin, P. Bloembergen, K. Anhalt, J. Hartmann, M. Sadli, P. Saunders, E. Woolliams, Y. Yamada, H. Yoon, Int. J. Thermophys. **31**, 1779 (2010)
 5. E.R. Woolliams, M.R. Dury, T.A. Burnitt, P.E.R. Alexander, R. Winkler, W.S. Hartree, S.G.R. Salim, G. Machin, Int. J. Thermophys. **32**, 1 (2011)
 6. H.W. Yoon, C.E. Gibson, G.P. Eppeldauer, A.W. Smith, S.W. Brown, K.R. Lykke, Int. J. Thermophys. **32**, 2217 (2011)
 7. V.R. Gavrilov, B.B. Khlevnoy, D.A. Otryaskin, I.A. Grigorieva, M.L. Samoylov, V.I. Sapritsky, in *Proceedings of Ninth International Temperature Symposium* (Los Angeles), *Temperature: Its Measurement and Control*, ed. by C.W. Meyer. Science and Industry, vol. 8, A.I.P. Conference Proceedings 1552 (AIP, Melville, NY, 2013), pp. 329–334
 8. J. Hartmann, Phys. Rep. **469**, 205 (2009)
 9. K.S. Wulfson, Zhurnal Eksperimental'noi i Teoreticheskoi Fiziki (J. Exp. Theor. Phys.) **21**, 507 (1951). [in Russian]
 10. V.I. Sapritskii, Metrologia **27**, 53 (1990)
 11. A.V. Prokhorov, S.N. Mekhontsev, V.I. Sapritsky, in *Proceedings of TEMPMEKO '99, 7th International Symposium on Temperature and Thermal Measurements in Industry and Science*, ed. by J.F. Dubbeldam, M.J. de Groot (Edauw Johannissen bv, Delft, 1999), pp. 698–703
 12. E.R. Woolliams, R. Winkler, S.G.R. Salim, P.M. Harris, I.M. Smith, Int. J. Thermophys. **30**, 144 (2009)
 13. P. Saunders, Int. J. Thermophys. **35**, 417 (2014)
 14. R.P. Madden, T.R. O'Brian, A.C. Parr, R.D. Saunders, V.I. Sapritsky, Metrologia **32**, 425 (1995/96)
 15. L.P. Boivin, C. Bamber, A.A. Gaertner, R.K. Gerson, D.J. Woods, E.R. Woolliams, J. Mod. Opt. **57**, 1648 (2010)
 16. A.F. Kotyuk, L.S. Lovinskii, L.N. Samoilo, V.I. Sapritskii, Meas. Tech. **18**, 75 (1975)
 17. B.B. Khlevnoi, Meas. Tech. **44**, 308 (2001)
 18. JCGM 101:2008. Evaluation of measurement data—Supplement 1 to the “Guide to the expression of uncertainty in measurement”—Propagation of distributions using a Monte Carlo method (JCGM: Joint Committee for Guides in Metrology, 2008)
 19. F. Sakuma, M. Kobayashi, in *Proceedings of TEMPMEKO '96, 6th International Symposium on Temperature and Thermal Measurements in Industry and Science*, ed. by P. Marcarino (Levrotto and Bella, Torino, 1997), pp. 305–310
 20. P. Saunders, D.R. White, Metrologia **40**, 195 (2003)
 21. W.H. Press, S.A. Teukolsky, W.T. Vetterling, B.P. Flannery, *Numerical Recipes: The Art of Scientific Computing* (Cambridge University Press, London, 1986)
 22. SCHOTT Optical Filter Glass. Properties (2013), http://www.schott.com/advanced_optics/english/download/schott-optical-filter-glass-properties-2013-eng.pdf. Accessed 13 November 2014
 23. S.A. Ogarev, B.B. Khlevnoy, M.L. Samoylov, V.I. Shapoval, V.I. Sapritsky, M.K. Sakharov, in *Proceedings of TEMPMEKO 2004, 9th International Symposium on Temperature and Thermal Measurements in Industry and Science*, ed. by D. Zvizdić, L.G. Bermanec, T. Veliki, T. Stašić (FSB/LPM, Zagreb, Croatia, 2004), pp. 569–574
 24. M. Clerc, *Particle Swarm Optimization* (Wiley-ISTE, London, 2006)
 25. J.J. Moré, B.S. Garbow, K.E. Hillstrome, User Guide for MINPACK-1. Report ANL-80-74 (Argonne National Laboratory, Argonne, IL, 1980), <http://cds.cern.ch/record/126569/files/CM-P00068642.pdf>. Accessed 14 Nov 2014
 26. J. Schwinger, Phys. Rev. **75**, 1912 (1949)
 27. J.R. Stevenson, H. Ellis, R. Bartlett, Appl. Opt. **12**, 2284 (1973)
 28. P.-S. Shaw, U. Arp, K.R. Lykke, Phys. Rev. Spec. Top. Accel. Beams **9**, 070701 (2006)
 29. R.D. Klein, R. Taubert, R. Thornagel, J. Hollandt, G. Ulm, Metrologia **46**, 359 (2009)
 30. R. Klein, R. Thornagel, G. Ulm, Metrologia **47**, R33 (2010)
 31. R.P. Brent, Comput. J. **14**, 422 (1971)
 32. R. Klein, G. Brandt, R. Fliegau, A. Hoehl, R. Müller, R. Thornagel, G. Ulm, M. Abo-Bakr, J. Feikes, M.V. Hartrott, K. Holldack, G. Wüstefeld, Phys. Rev. Spec. Top. Accel. Beams **11**, 110701 (2008)
 33. R. Klein, G. Brandt, R. Fliegau, A. Hoehl, R. Müller, R. Thornagel, G. Ulm, M. Abo-Bakr, K. Buerkmann-Gehrlein, J. Feikes, M.V. Hartrott, K. Holldack, J. Rahn, in *Proceedings of EPAC'08—11th European Particle Accelerator Conference* (Genoa, Italy, 2008), pp. 2055–2057